ISSN 0725-783X

ELECTRON MOMENTUM SPECTROSCOPY

I.E. McCarthy

FIAS-R-170

MARCH 1986

ELECTRON MOMENTUM SPECTROSCOPY

I.E. McCarthy,

Institute for Atomic Studies, The Flinders University of South Australia, Bedford Park, S.A. 5042, Australia.

ABSTRACT

For sufficiently-high electron energies (greater than a few hundred eV) and sufficiently-low recoil momenta (less than a few atomic units) the differential cross section for the non-coplanar-symmetric (e,2e) reaction on an atom or molecule depends on the target and ion structure only through the target-ion overlap. Experimental criteria for the energy and momentum are that the appa.ent structure information does not change when the energy and momentum are varied. The plane-wave impulse approximation is a sufficient description of the reaction mechanism for determining spherically-averaged squares of momentum-space orbitals for atoms and molecules and for coefficients describing initial- and final-state correlations. For mainly-uncorrelated initial states spectroscopic factors for final states belonging to the same manifold are uniquely determined. For molecules summed spectroscopic factors can be compared for different ion manifolds. For atoms summed spectroscopic factors and higher-momentum profiles require the distorted wave impulse approximation.

Submitted to Australian Journal of Physics

1. INTRODUCTION

This talk is about the relationship of the non-coplanar symmetric (e,2e) reaction (McCarthy and Weigold 1976) to quantum chemistry. It is a very direct relationship. We will see how this comes about and illustrate it with pertinent examples. Throughout the talk I will use some terms in senses related to the experiment and described schematically in fig. 1.

Energy E

$$E = E_A + E_B = E_0 - \epsilon_f . \qquad (1)$$

Momentum p,

$$\underline{p} = \underline{k}_A + \underline{k}_B - \underline{k}_0 . \qquad (2)$$

The separation energy ϵ_f of the electronic state of the final ion and the momentum p are directly measured by the experiment as is the relative differential cross section, spherically averaged over target orientations.

$$\frac{d^5\sigma}{d\Omega_A d\Omega_B dE_A} = (2\pi)^4 \frac{k_A k_B}{k_0} (4\pi)^{-1} \int d\hat{p} |T_f|^2 . \qquad (3)$$

Momentum profile means the shape of the curve of the differential cross section plotted against the ion recoil momentum p.

Polar angle θ means the angle made by each of $\underline{k}_0, \underline{k}_A$ and $\underline{k}_B$ with the incident direction $\hat{\underline{k}}_0$. It is close to 45° to maximise the momentum transfer and minimise p when $\underline{k}_0, \underline{k}_A$ and $\underline{k}_B$ are

coplanar.

Azimuthal angle ϕ means the azimuthal angle of $\underline{k}_B$ relative to the $\underline{k}_0\underline{k}_A$ plane. This is varied from zero to about 30° in order to vary p from 0 to 2 or 3 atomic units (called low momentum) at energies E of the order of a kilovolt (called high energy, since it is many times ϵ_f for the valence states under consideration).

A quantum chemist is a person who believes in the Schrodinger equation. He believes that if his methods, such as variational calculations, configuration interaction and Green's functions, are used hard enough and long enough all will be revealed. Unfortunately the (e,2e) reaction can't be treated by these methods. We can't even begin to solve the Schrodinger equation because we don't know the boundary conditions for three bodies with Coulomb interactions. This is why some quantum chemists find it difficult and mysterious. Yet I believe that the high energy, low momentum (e,2e) reaction is understood better than any other reaction in atomic or nuclear physics in the sense that we can calculate right answers with more certainty. Is this because we reaction theorists are computational geniuses? No, it is because the experimentalist has done nearly all the work. He measures enough simultaneous quantities to enable us to focus our thoughts on a kinematic range where quite a simple treatment of the reaction based on an understanding of probability amplitudes is sufficient. This simple treatment relates the reaction very directly to the quantum chemical structure of the target atom or molecule and the ion. Perhaps more importantly the experimentalist can verify the validity of the relationship by checking that the apparent structure information is independent of energy and hence of the

part of the calculation dependent on the reaction conditions.

2. INTUITIVE REACTION THEORY

The amplitude for an (e,2e) reaction leading from the target ground state g to a final ion state f is

$$T_f(\underline{k}_0,\underline{k}_A,\underline{k}_B) = \langle \underline{k}_A \underline{k}_B f|T|g\underline{k}_0\rangle, \qquad (4)$$

where T is the (unknown) transition operator that gives the correct amplitude. We first make a simple and experimentally-verifiable approximation.

The binary-encounter approximation.

The transition operator T is approximated by a three-body operator depending on the coordinates of the incident and struck electrons and the centre of mass of the residual ion, but not explicitly on the coordinates of the remaining electrons. With this approximation the (e,2e) amplitude becomes

$$T_f(\underline{k}_0,\underline{k}_A,\underline{k}_B) = \int d^3q \langle \underline{k}_A \underline{k}_B|T|\underline{q}\ \underline{k}_0\rangle\langle \underline{q}f|g\rangle. \qquad (5)$$

The vitally important thing about the form (5) is that T_f now depends on the structure wave functions f of the ion and g of the target ground state only through the target-ion overlap $\langle \underline{q}f|g\rangle$. This quantity is directly calculated by the methods of quantum chemistry, so that (5) constitutes the relationship between the reaction and quantum chemistry. Its verification depends on whether apparent structure information is independent of energy E

We can form some a priori idea of the conditions for the validity of (5). Some of the terms it neglects are exchange terms involving the overlap of a continuum and a bound-state orbital for a particular electron. These overlaps are vanishingly-small for electron energies of several hundred eV and valence orbitals. This gives a lower limit on E.

The first amplitude in the integrand of (5) describes the reaction mechanism. We must make further approximations to it in order to calculate the differential cross section. The simplest approximation is that T just describes the collision of the two electrons. It then becomes the electron-electron t-matrix

$$\begin{aligned} \langle \underline{k}_A \underline{k}_B | T | \underline{q}\ \underline{k}_0 \rangle &= \langle \underline{k}' | t(E) | \underline{k} \rangle \delta(\underline{q} - \underline{k}_A - \underline{k}_B + \underline{k}_0), \\ \underline{k}' &= \tfrac{1}{2}(\underline{k}_A - \underline{k}_B), \\ \underline{k} &= \tfrac{1}{2}(\underline{q} - \underline{k}_0), \\ \underline{q} &= \underline{p}. \end{aligned} \qquad (6)$$

This is the plane-wave impulse approximation (PWIA). Note that (5) now factorises into the target-ion overlap $\langle \underline{p}f | g \rangle$ calculated at the experimental momentum $\underline{p}$ and an electron-electron collision factor which is essentially the Mott scattering amplitude except that $\underline{k}'$ corresponds to the experimental energy E but $\underline{k}$ does not. It is half-off-shell, but all momenta are measured in the experiment. When summed and averaged over electron spin states the electron-electron factor in the cross section becomes (Chen and Chen 1972)

$$f_{ee} = \frac{1}{(2\pi^2)^2}\frac{2\pi\nu}{\exp(2\pi\nu)-1}\left\{\frac{1}{|\underline{k}_0-\underline{k}_A|^4}+\frac{1}{|\underline{k}_0-\underline{k}_B|^4}-\frac{1}{|\underline{k}_0-\underline{k}_A|^2}\frac{1}{|\underline{k}_0-\underline{k}_B|^2}\right.$$
$$\left.\times\cos\left[\nu\,\ell n\,\frac{|\underline{k}_0-\underline{k}_B|^2}{|\underline{k}_0-\underline{k}_A|^2}\right]\right\}$$

$$\nu = 1/|\underline{k}_A-\underline{k}_B|, \qquad (7)$$

and the cross section is

$$\frac{d^5\sigma}{d\Omega_A d\Omega_B dE_A} = (2\pi)^4\frac{k_A k_B}{k_0}f_{ee}(4\pi)^{-1}\int d\hat{p}\,|\langle \underline{p}f|g\rangle|^2. \qquad (8)$$

In fact we expect that momentum can be transferred by elastic scattering in each two-electron subsystem. It is computationally feasible to take this into account by retaining the factorisation implied by (6) but replacing the plane waves $|\underline{k}_A>$, $|\underline{k}_B>$ and $|\underline{k}_0>$ in $\langle \underline{q}f|g\rangle$ by elastic scattering states $|\chi^{(-)}(\underline{k}_A)>$, $|\chi^{(-)}(\underline{k}_B)$ and $|\chi^{(+)}(\underline{k}_0)>$ calculated in the appropriate two-body potential. In fact we use the static-exchange potential of one electron and the ion for the final state and that of one electron and the target for the initial state. This gives us the distorted-wave impulse approximation (DWIA)

$$\frac{d^5\sigma}{d\Omega_A d\Omega_B dE_A} = (2\pi)^4\frac{k_A k_B}{k_0}f_{ee}(4\pi)^{-1}\int d\hat{p}\,|\langle\chi^{(-)}(\underline{k}_A)\chi^{(-)}(\underline{k}_B)f|g\chi^{(+)}(\underline{k}_0)\rangle|^2, \qquad (9)$$

which is the reaction theory that gives a complete understanding of the reaction under the high-energy low-momentum conditions of EMS for atomic targets. For molecular targets it is difficult to calculate the distorted waves, but our complete understanding

enables us to identify experimental conditions under which the PWIA (8) is valid and gives the same structure information.

3. COMPARISON WITH PHOTOELECTRON SPECTROSCOPY

Since the subject of this session is the comparison of EMS with photoelectron spectroscopy (PES) it is appropriate at this stage to make some comparisons for reactions in which (e,2e) is experimentally feasible (McCarthy 1985). At present this covers stable gas targets and energy resolution $\Delta E \sim 1eV$. Solid or transient-gas targets and higher energy resolution are at present the exclusive province of PES, although this is changing.

It is sometimes claimed that PES gives valuable structure information about valence states. Indeed there is a superficial resemblance to EMS in that both observe the energies of electronic states of the ion. However here the resemblance ends. PES obviously contains structure information, but it is in a very convoluted form involving a heroic computational effort to describe differential cross sections that, for the spectroscopic application, are only now beginning to be reliably measured.

The major theoretical problem is inherent in the two-body kinematics of the reaction. The energy E is uniquely related to the momentum by

$$E = \tfrac{1}{2}p^2. \qquad (10)$$

Thus the high-energy, low-momentum condition is unattainable. The reaction involves a difficult (but possible) calculation at low energy, using a continuum electron function derived from a calculation involving channel coupling and electron correlation

(e.g. Berrington et al. 1980). However at high energy and momentum ($p \sim 10$) the plane-wave approximation for the continuum electron is invalidated by the strong short-distance electron-ion potential and there is a new amplitude in the calculation beyond the usual dipole approximation, that becomes non-negligible at such momenta (Amusia and Kheifets 1985).

4. ONE-ELECTRON CHEMISTRY

The (e,2e) reaction is a direct observation of the target-ion overlap $\langle \underline{p}f|g\rangle$, under the conditions of validity of the PWIA. Under conditions that are realistic for most targets it takes a particularly simple form.

For the hydrogen atom

$$|\langle \underline{p}f|g\rangle|^2 = |\phi(p)|^2 = (2^3/\pi^2)(1+p^2)^{-4} \qquad (11)$$

This momentum profile is verified for different energies in fig. 2, thus verifying the validity of the assumptions involved in the PWIA (8).

For the helium atom the overlap can be fully evaluated very easily using a converged configuration-interaction (CI) wave function for g and the (hydrogenic) wave functions of He^+. For the 1s state the momentum profile is the same as that obtained using the He Hartree-Fock function as an approximation to $\langle \underline{p}f|g\rangle$ over several orders of magnitude. Initial-state correlations result in excitation of $n=2$ and higher states of He^+. The $n=2$ momentum profile relative to the 1s profile is shown in fig. 3.

For larger targets we represent $|g\rangle$ as a CI expansion in Slater determinants $|\alpha\rangle$ of target Hartree-Fock orbitals.

$$|g\rangle = \Sigma_\alpha e_\alpha |\alpha\rangle. \tag{12}$$

In order to use orthonormality we also represent the ion in terms of target Slater determinants $|\beta\rangle$ coupled with appropriate symmetry to one-hole states ϕ_j, whose symmetry is indicated by a quantum number set j. Final ion states f_m belonging to a symmetry manifold indicated by m are expanded as

$$|f_m\rangle = \Sigma_{j\beta} \, t_{j\beta}^{(f)} C_{jm\beta} \phi_j^\dagger |\beta\rangle. \tag{13}$$

We normally consider final states belonging to a particular symmetry manifold m and thus drop the subscript m from f.

The overlap $\langle \underline{p} f|g\rangle$ is, in the common case $a_o \sim 1$ for closed-shell targets,

$$\langle \underline{p} f|g\rangle = N^{\frac{1}{2}} t_{j0}^{(f)} \psi_j(\underline{p}), \tag{14}$$

where orbitals with the same symmetry j sum to a function $\psi_j(\underline{p})$ called the characteristic orbital. As in the case of helium $\psi_j(\underline{p})$ is essentially a target Hartree-Fock orbital. The factor $N^{\frac{1}{2}}$, where N is the occupation number of the target orbital ψ_j, is introduced by antisymmetrization (Cook et al. 1986). The square of the spectroscopic amplitude $t_{j0}^{(f)}$ is the spectroscopic factor $S_j^{(f)}$. It represents the probability that f consists of the one-

hole configuration $\Psi_j^{\dagger}|0\rangle$.

The spectroscopic sum rule

$$\Sigma_f S_j^{(f)} = 1. \qquad (15)$$

obtained from the orthonormality and closure relations for the manifold defined by the symmetry j, enables us to make a one-electron theory of the (e,2e) reaction which amounts to an experimental definition of an orbital for a manifold j.

1. The orbital momentum profile $\int d\hat{p}|\Psi_j(\underline{p})|^2$ is given by the (e,2e) profile. Note that for EMS f_{ee} is essentially independent of p.

2. The magnitude of the orbital differential cross section is given by the sum of cross sections for reactions to states f in the manifold j.

3. The orbital energy is obtained from the orthonormality and closure relations as the manifold centroid

$$\epsilon_j = \Sigma_f S_j^{(f)} \epsilon_f. \qquad (16)$$

5. THE UNDERSTANDING AFFORDED BY THE DWIA

If we make the approximation that the target ground state $|g\rangle$ can be represented by the target Hartree-Fock determinant $|0\rangle$, we can substitute the one-electron overlap (14) in the expression (9)

to obtain the target Hartree-Fock DWIA (THF-DWIA).

$$\frac{d^5\sigma}{d\Omega_A d\Omega_B dE_A} = (2\pi)^4 \frac{k_A k_B}{k_0} f_{ee} \, NS_j^{(f)} \times (4\pi)^{-1} \int d\hat{p} \, |\langle \chi^{(-)}(\underline{k}_A) \chi^{(-)}(\underline{k}_B) | \Psi_j \chi^{(+)}(\underline{k}_0) \rangle|^2 . \qquad (17)$$

Note that the THF approximation involves the neglect of initial-state-correlation effects, which we illustrated for helium in fig. 3. They are usually of the order of a few percent.

The first illustration is the 3p manifold of Ar^+, which involves negligible final-state correlations. The THF-DWIA agrees perfectly with the experimental cross section (normalised at 7.5°) in fig. 4. Note that the polar angle θ in this experiment is 47°. The theoretical description is good here, even though the small-ϕ shape of the PWIA is not correct in detail for the 3p profile. The flatter profile for small ϕ enables the effect of finite angular resolution to be neglected.

Fig. 5 for the 3s manifold delivers the illustration of the full power of DWIA analysis. Not only is the profile shape correct. Its magnitude (remembering that the whole experiment has already been normalised for fig. 4) is correct and the spectroscopic factor $S_{3s}^{(29.3)}$ of the strongest state at 29.3 eV is found to be 0.55±0.02 by two independent methods, use of the sum rule (15) within the 3s manifold, and direct comparison of the 29.3eV cross section with the 3p cross section. Note that the low-momentum shape of the 3s profile is given adequately by the

PWIA. This has been used to assign spectroscopic factors within the 3s manifold. Momentum profiles for 3s states are shown in fig. 6.

We can find the optimum polar angle θ for the PWIA by considering the cross section in the Φ=0 plane as a function of θ. This is illustrated in fig. 7 for the Ar 3p case. The plane-wave minimum is shifted to the left of 45° by the finite separation energy. The distorted-wave minimum is shifted to the right by about the same amount since the average distorting potential is comperable with the separation energy. The plane-wave and distorted-wave cross sections agree at 45°. This argument holds approximately for all orbitals so the optimum angle for the PWIA is 45°.

Figs. 8 and 9 (for θ=45°) show the comparison for the 5p and 5s manifolds of xenon analogous to figs. 4 and 5 for argon. Here the Dirac-Fock orbitals are used in preference to Hartree-Fock. Fig. 10 shows that the correct ratio of $5p_{3/2}$ to $5p_{1/2}$ cross sections is obtained. The one-electron analysis is completely confirmed. In addition the PWIA and DWIA agree in shape detail up to p~1.5 for 5p and 1.0 for 5s, both of which are large enough momenta for the main features of the profiles to be observed, and in particular for assignment of manifold symmetry. This comparison affords a verification of the use of the PWIA at θ=45° to give detailed low-momentum profiles.

Final confirmation of the one-electron analysis is given by the orbital energy (16) of the argon 3s manifold, which is 34.5±0.2 eV in agreement with Hartree-Fock and of the xenon 5s manifold,

which is
eV.

6. THE
The
for ato
the use

Fig
electro
profile
indicat
are con
necessa
section
rule.
maximu
example
Taking
agreeme

Fi
overla
1977),
orbita
attrib
precis

which is 27.6±0.3 eV in agreement with the Dirac-Fock value 27.5 eV.

6. THE PWIA FOR MOLECULES

The understanding of the (e,2e) reaction that we have obtained for atoms leads to the conclusion that the optimum conditions for the use of the PWIA for molecules are E~1000 eV, θ=45°.

Fig. 11 for ethane illustrates the main features of the one-electron THF-PWIA analysis. First the summed manifold momentum profiles all agree with experiment in relative magnitude, indicating that spectroscopic factor assignments within manifolds are confirmed by comparing manifold sums. It is of course not necessary to measure the one unknown number that would make cross sections absolute. Normalisation is done by the spectroscopic sum rule. The analysis is valid for E=400 eV and 1200 eV up to maximum momenta p_{max} that vary with E and the manifold. For example p_{max} is 0.9 for $2a_{1g}$ at 400 eV and 1.2 for 1200 eV. Taking account of angular resolution improves the small-Φ agreement.

Fig. 12 for water shows that a direct calculation of the overlap, in this case by Green's function methods (Dixon et al 1977), improves on profile shapes given by medium-quality SCF orbitals. The low-momentum disagreement for the $1b_1$ orbital is attributed to inadequate structure calculations in view of the precise agreement for other cases.

7. CORRELATIONS WITHIN AN INNER-VALENCE MANIFOLD

Spectroscopic factors are precisely assigned by EMS to the fragments of an orbital constituting an inner-valence manifold. So far this has provided the toughest challenge to quantum chemistry, and until recently direct CI methods gave only qualitatively-correct relative magnitudes while Green's function methods have been less successful.

The simplest non-trivial test case is the 3s manifold of argon, since the fragements are well-separated and precisely assigned, (see fig. 6). Large-basis direct CI calculations by Mitroy, Amos and Morrison (1984) obtained 0.60 for the largest spectroscopic factor in comparison with the experimental value 0.55±0.02. A Green's function calculation of the overlap amplitude by Amusia and Kheifets (1985) gives improved spectroscopic factors. The comparison with experiment is given in Table I.

A recent direct CI calculation by the Perugia group (Sgamellotti 1986) for Cl_2 involved about 100,000 configurations for the inner-valence manifolds. Separation energies and relative spectroscopic factors agree closely with experiment for the first two of three large fragments of the $4\sigma_u$ manifold that are clearly observable. There are indications that calculations of this order of magnitude are necessary to obtain an adequate quantum-chemical description of the spectroscopic-factor aspect of electron correlations.

REFER
Amus
Berr
J.Phy
Chen
Cook
Phys
Dey,
J.El
Dixo
G.R.
Lohm
McCa
McCa
McCa
Mitr
165
Mitr
414

REFERENCES

Amusia, M.Ya., and Kheifets, A.S (1985) J.Phys.B 18, L679.

Berrington, K.A., Burke, P.G., Fon, W.C. and Taylor, K.T. (1980). J.Phys.B 15, L603.

Chen, J.C.Y., and Chen, A.C. (1972). Adv.At.Mol.Phys.8, 71.

Cook, J.P.D., McCarthy, I.E., Mitroy, J.D., and Weigold, E. (1986). Phys.Rev.A 33, 211.

Dey, S., Dixon, A.J., McCarthy, I.E. and Weigold, E. (1976). J.Elec.Spectrosc. 9, 397.

Dixon, A.J., Dey, S., McCarthy, I.E., Weigold, E. and Williams, G.R.J. (1977). Chem.Phys. 21, 81.

Lohmann, B. and Weigold, E. (1981). Phys.Lett.A 86, 139.

McCarthy, I.E. (1985). J.Elec.Spectr. 36, 37.

McCarthy, I.E. and Weigold, E. (1976). Phys.Rep. 27C, 275.

McCarthy, I.E. and Weigold, E. (1985). Phys.Rev.A 31, 160.

Mitroy, J.D., Amos, K.A. and Morrison, I. (1984). J.Phys.B 17, 1659.

Mitroy, J.D., McCarthy, I.E. and Weigold, E. (1985). J.Phys.B 18, 4149.

Sgamellotti, A. (1986). Private communication.

Table I. Spectroscopic factors for the 3s-manifold of the argon ion. AK indicates the Green's function calculation of Amusia and Kheifets (1985). MAM indicates the direct CI calculation of Mitroy, Amos and Morrison (1984). EXP indicates experimental values (McCarthy and Weigold 1985).

ϵ(eV)	Assignment	AK	MAM	EXP
29.3	$3s3p^6$	0.55	0.600	0.547±0.019
36.7	$3s^2 3p^4 4s$	-	0.019	0.032±0.008
38.6	$3s^2 3p^4 3d$	0.20	0.142	0.175±0.011
41.2	$3s3p^4 3d$	0.11	0.075	0.074±0.007
42-43.4	3s3p 5d	0.04	0.095	0.041±0.006
>43.4	-	-		0.122±0.008

FIGURE CAPTIONS

Fig. 1 Schematic diagram defining the kinematic variables used in the description of the (e,2e) reaction.

Fig. 2 The momentum profile at different energies for the (e,2e) reaction on the hydrogen atom (Lohmann and Weigold 1981).

Fig. 3 The ration of n=2 to n=1 cross sections for the (e,2e) reaction on helium compared with the PWIA using a converged configuration-interaction function for the ground state (Mitroy et al. 1985).

Fig. 4 The DWIA and PWIA compared with 1000 eV (e,2e) data at θ=47° for the 3p orbital of argon (McCarthy and Weigold 1985). The experiment is normalized to the curve at 7.5°.

Fig. 5 The DWIA and PWIA compared with 1000 eV (e,2e) data at θ=47° for the 29.3 eV state of Ar^+ (crosses) and the 3s manifold sum (filled circles). The normalisation is the same as for Fig. 14. The DWIA curve for the 29.3 eV state includes a spectroscopic factor of 0.55 (McCarthy and Weigold 1985).

Fig. 6 Momentum profiles for different ion states in the 3s manifold for the (e,2e) reaction on argon at the indicated energies (McCarthy and Weigold 1976). The curve in every case is the 3s Hartree-Fock PWIA.

Fig. 7 The PWIA and DWIA for the 1000 eV (e,2e) reaction on argon for ϕ=0 and varying θ near the low-momentum minimum.

Fig. 8 The DWIA and PWIA compared with 1000 eV (e,2e) data at θ=45° for the summed 5p orbitals of xenon (Cook et al 1986). The experiment is normalised to the curve at 5°

Fig. 9 The DWIA and PWIA compared with 1000 eV (e,2e) data at θ=45° for the 5s manifold sum of xenon. The normalisation is the same as for Fig. 8.

Fig. 10 The DWIA and PWIA calculations of the ration of $5p_{3/2}$ to $5p_{1/2}$ cross sections for the 1000 eV (e,2e) reaction on xenon (Cook et al 1986).

Fig. 11 Momentum profiles for the valence orbitals of ethane analysed with the PWIA and Hartree-Fock functions (Dey et al 1976).

Fig. 12 Momentum profiles for the valence orbitals of water compared with the PWIA using different calculations of $\underline{<}qf|g>$ (Dixon et al 1977). The full line is the overlap amplitude calculated by Green's function methods. Broken lines use molecular orbitals with different basis sets.

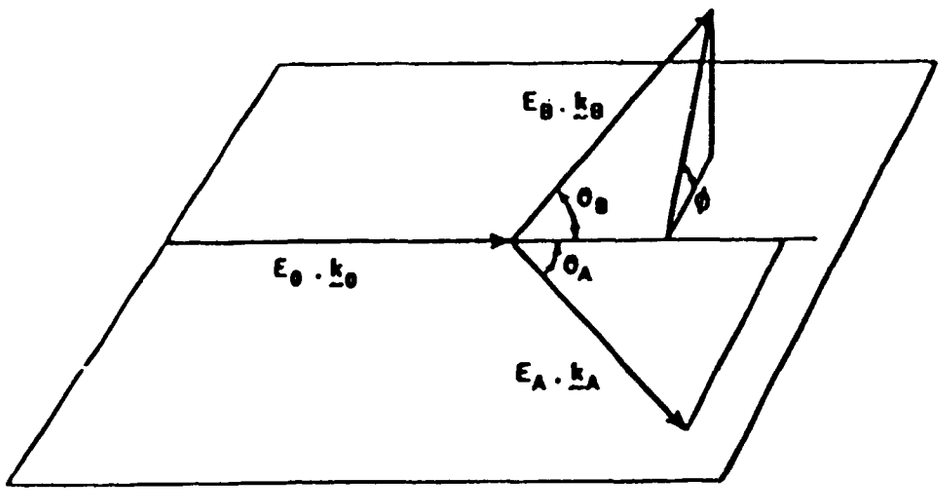
$E_B \cdot \underline{k}_B$
θ_B
ϕ
$E_0 \cdot \underline{k}_0$
θ_A
$E_A \cdot \underline{k}_A$

Fig. 1

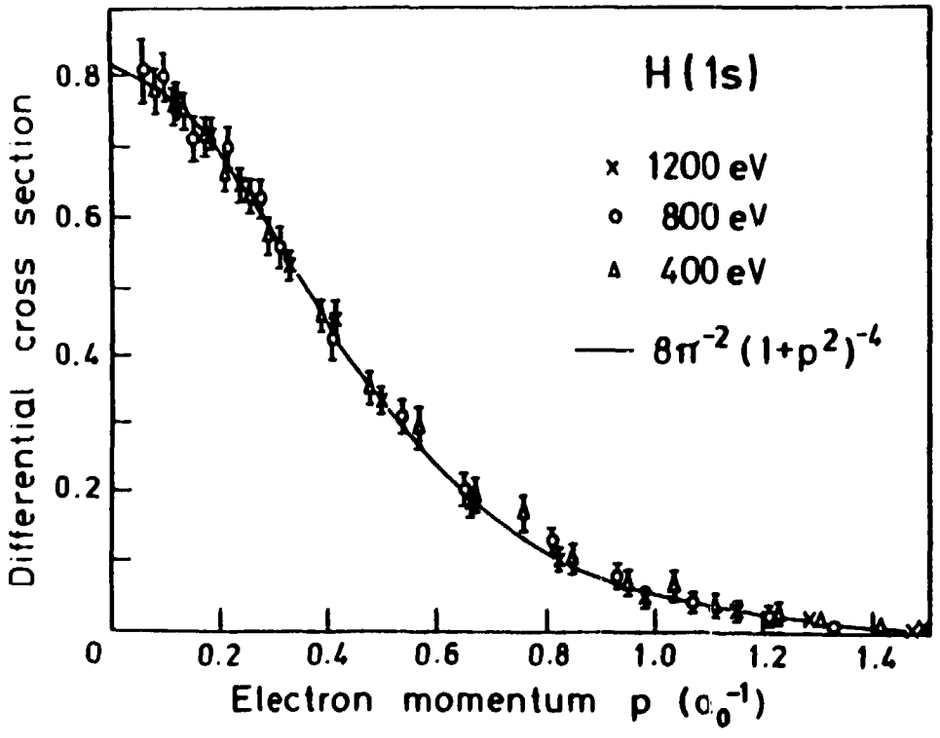
H (1s)
x 1200 eV
o 800 eV
Δ 400 eV
$8\pi^{-2}(1+p^2)^{-4}$
Differential cross section
0.8
0.6
0.4
0.2
0
0.2
0.4
0.6
0.8
1.0
1.2
1.4
Electron momentum p (a_0^{-1})

Fig. 2

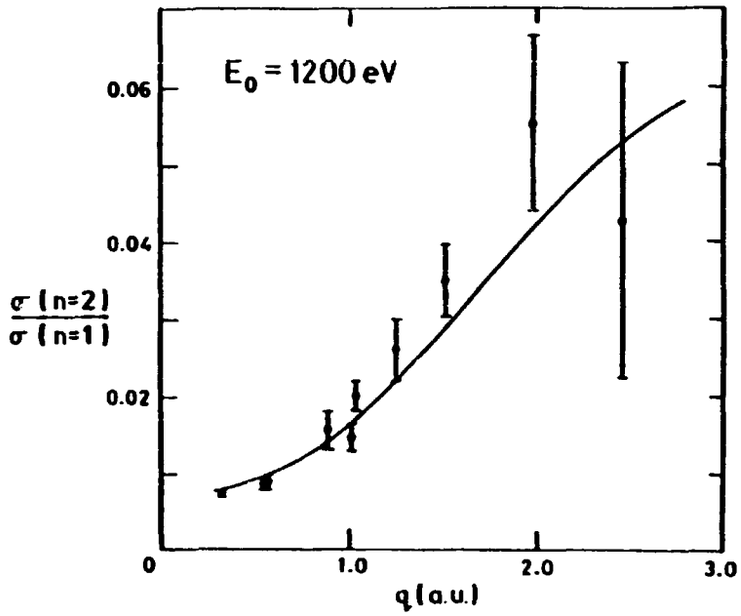
$E_0 = 1200$ eV
0.06
0.04
0.02
0
1.0
2.0
3.0
q (a.u.)
$\frac{\sigma(n=2)}{\sigma(n=1)}$

Fig. 3

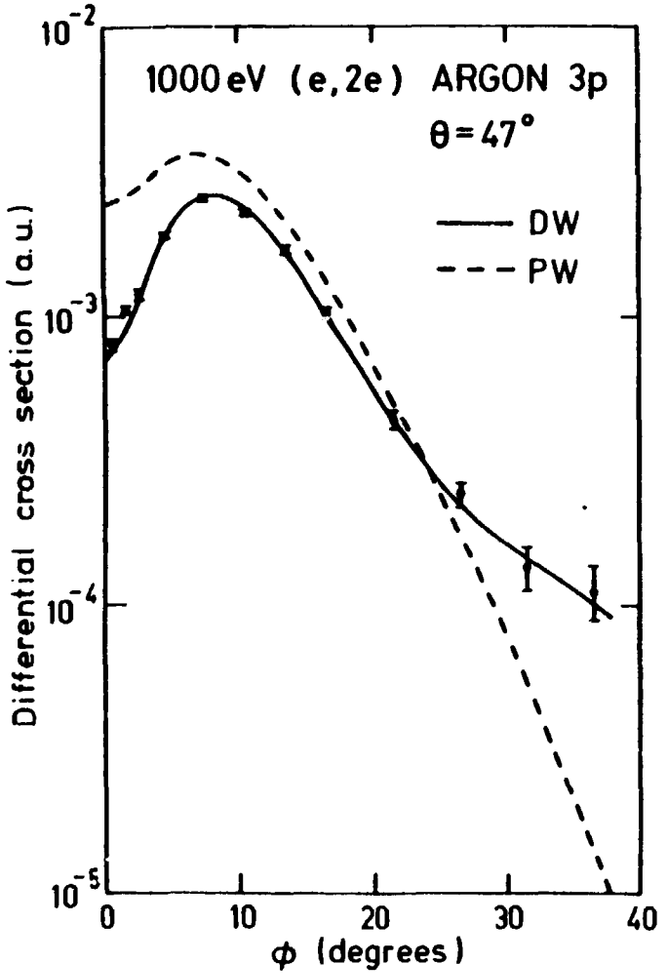
1000 eV (e,2e) ARGON 3p
θ = 47°
DW
PW
10^{-2}
10^{-3}
10^{-4}
10^{-5}
Differential cross section (a.u.)
0
10
20
30
40
φ (degrees)

Fig. 4

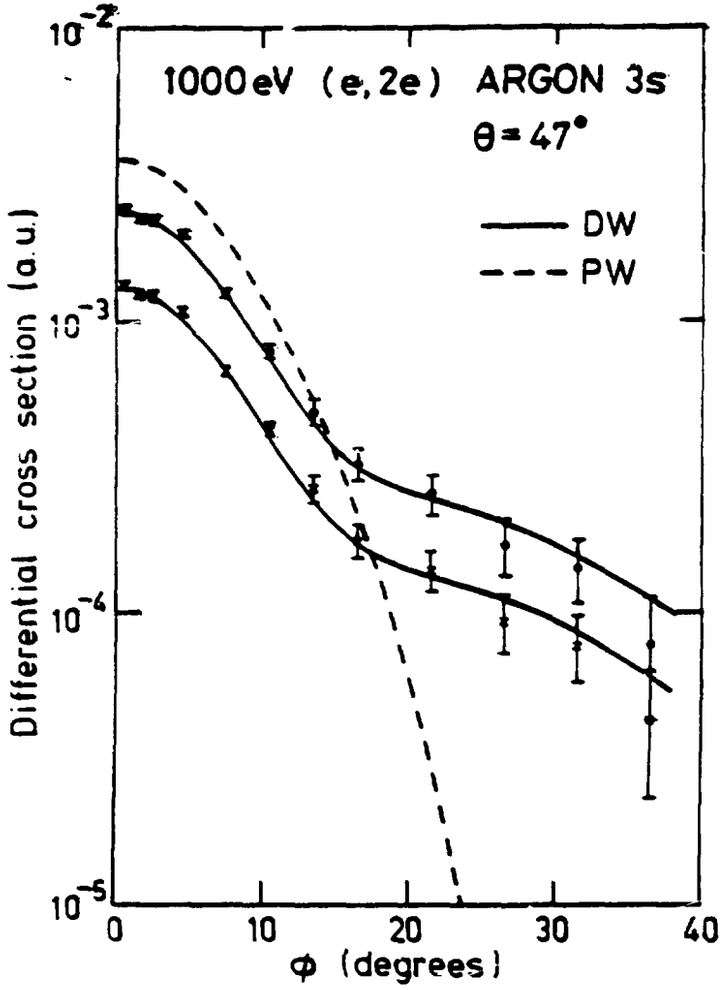
1000 eV (e, 2e) ARGON 3s
θ = 47°
DW
PW
Differential cross section (a.u.)
10^-2
10^-3
10^-4
10^-5
0
10
20
30
40
Φ (degrees)

Fig. 5

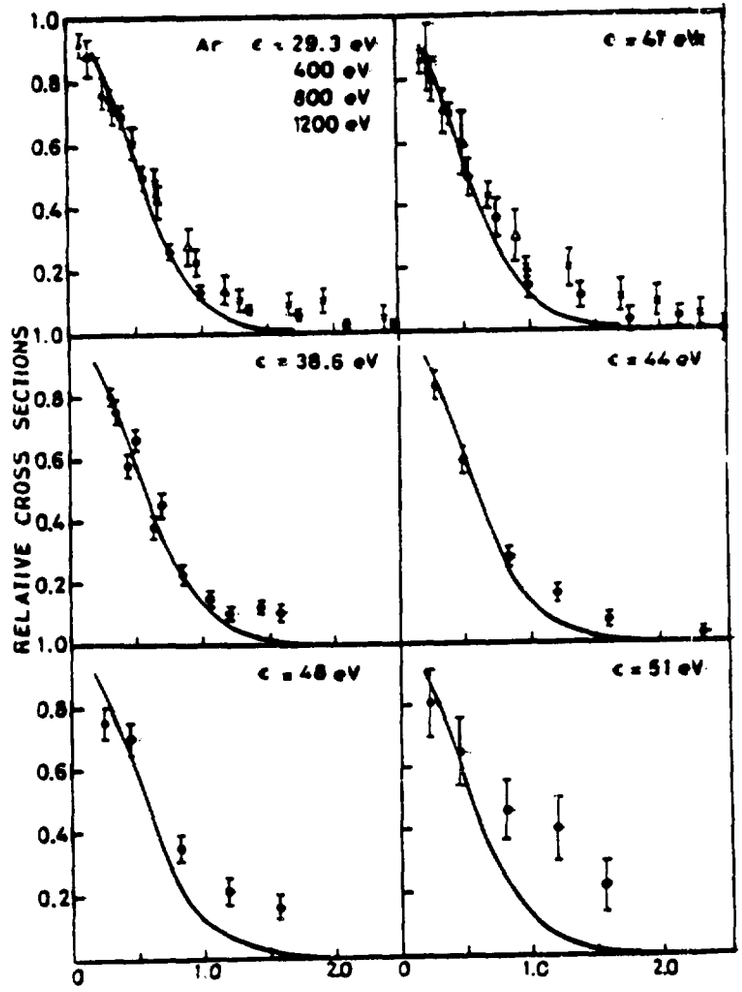
Ar
400 eV
800 eV
1200 eV
ε = 38.6 eV
ε = 44 eV
ε = 48 eV
ε = 51 eV
RELATIVE CROSS SECTIONS
1.0
0.8
0.6
0.4
0.2
0
1.0
2.0

Fig. 6

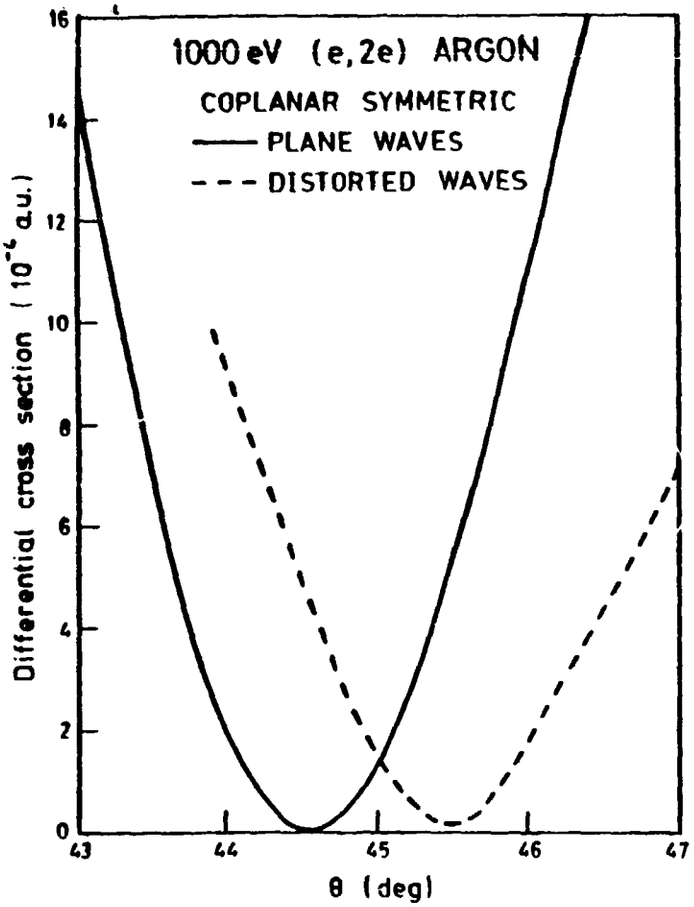
1000 eV (e,2e) ARGON
COPLANAR SYMMETRIC
PLANE WAVES
DISTORTED WAVES
Differential cross section (10^{-4} a.u.)
θ (deg)
0
2
4
6
8
10
12
14
16
43
44
45
46
47

Fig. 7

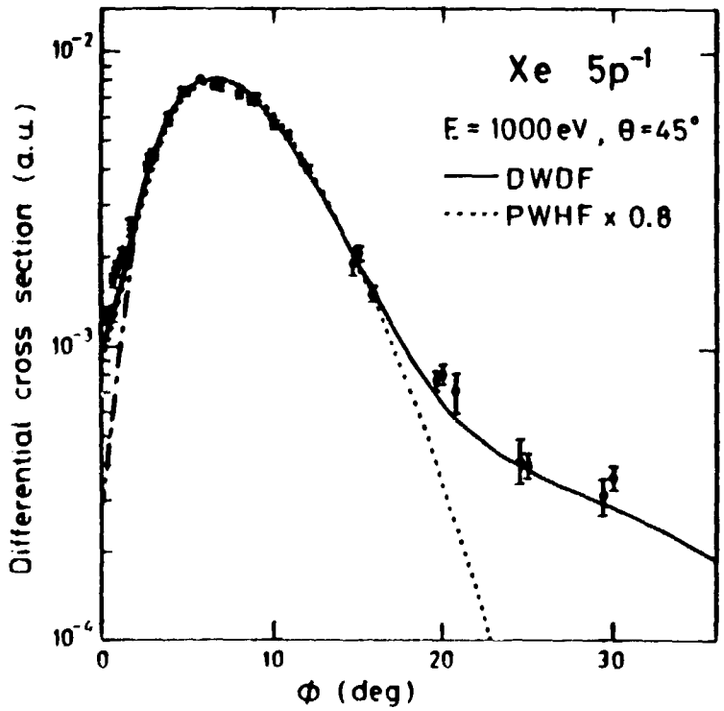
Xe $5p^{-1}$
E = 1000 eV , θ=45°
DWDF
PWHF x 0.8
Differential cross section (a.u.)
Φ (deg)
10^{-2}
10^{-3}
10^{-4}
0
10
20
30

Fig. 8

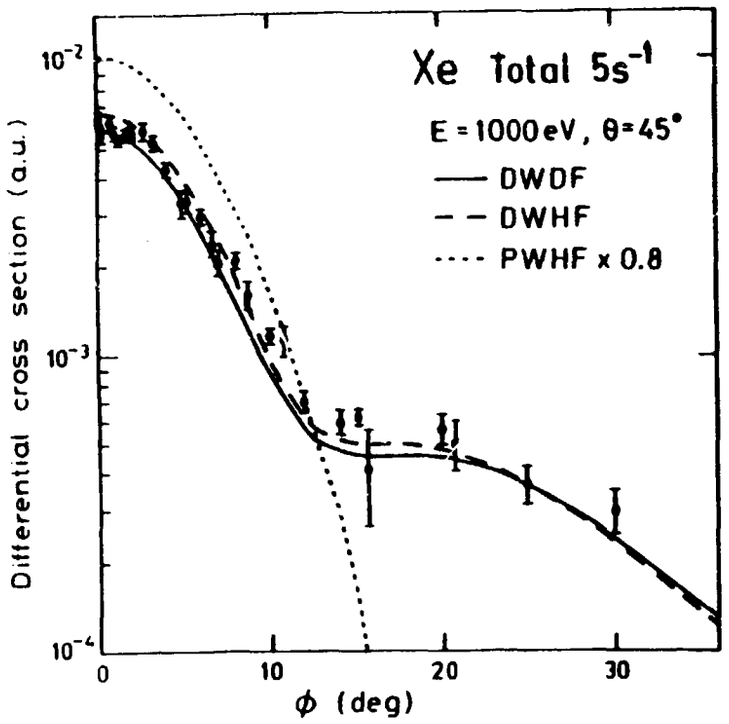
Xe Total 5s^{-1}
E = 1000 eV, θ = 45°
DWDF
DWHF
PWHF x 0.8
Differential cross section (a.u.)
10^{-2}
10^{-3}
10^{-4}
0
10
20
30
φ (deg)

Fig. 9

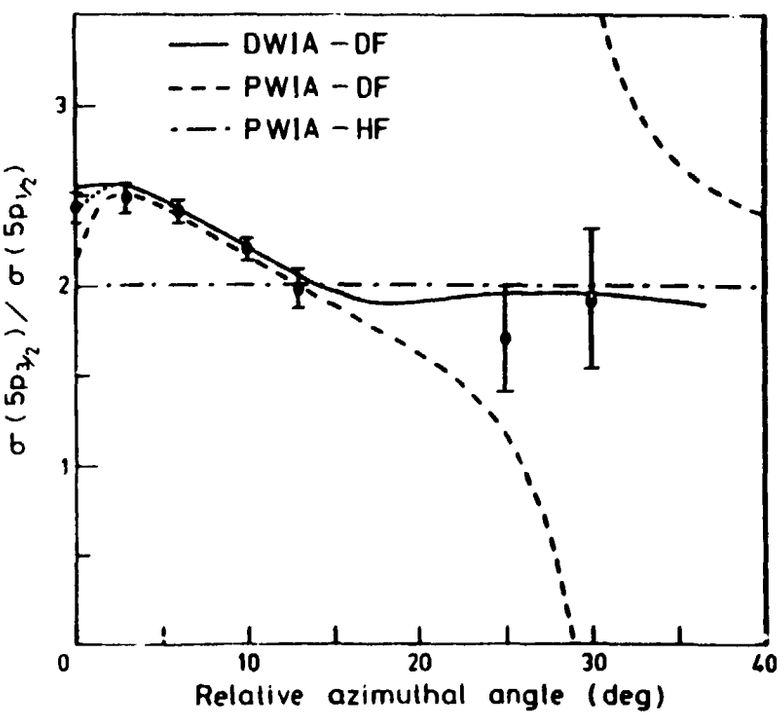
DWIA – DF
PWIA – DF
PWIA – HF
σ (5p3/2) / σ (5p1/2)
3
2
1
0
10
20
30
40
Relative azimuthal angle (deg)

Fig. 10

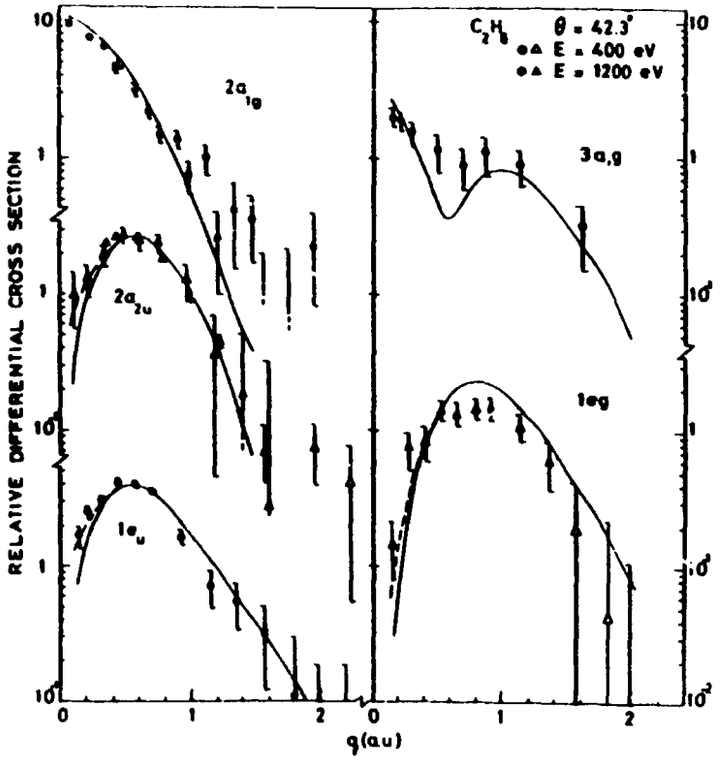
RELATIVE DIFFERENTIAL CROSS SECTION
C_2H_6 θ = 42.3°
E = 400 eV
E = 1200 eV
$2a_{1g}$
$2a_{2u}$
$1e_u$
$3a_g$
$1e_g$
q(au)

Fig. 11

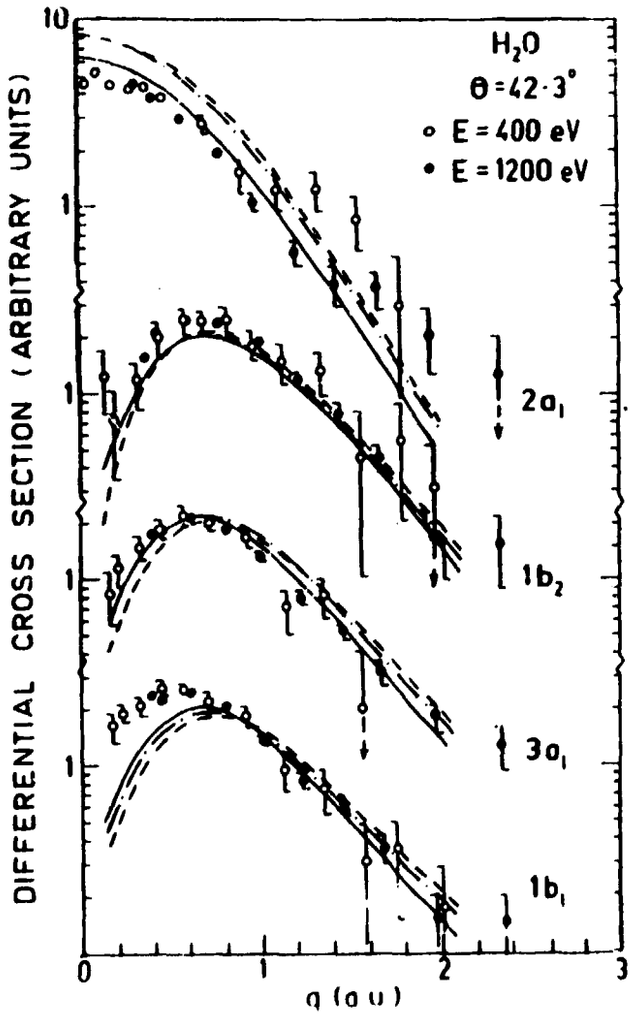
H_2O
θ = 42·3°
E = 400 eV
E = 1200 eV
DIFFERENTIAL CROSS SECTION (ARBITRARY UNITS)
$2a_1$
$1b_2$
$3a_1$
$1b_1$
q (a u)

Fig. 12